Title: Adjuvant Effects of Amphipathic Helical Peptides

Jyun-Hong Lyu[1], Guun-Guang Liou[2,3], May Wang[1], Ming-Chung Kan[1,4]

1. Vaxsia Biomedical Inc. 11503 Taipei, Taiwan
2. Institute of Biological Chemistry, Academia Sinica, 11529 Taipei, Taiwan
3. Office of Research and Development, College of Medicine, National Taiwan University, 10051 Taipei, Taiwan
4. Corresponding author

Abstract

Subunit vaccine is the focus of research in developing new vaccines against infectious disease. Due to the low immunogenicity of recombinant protein, adjuvant are required for the activation of humoral and cellular immunity against an protein antigen. In this study, we reported the identification of a novel pathway that can activate humoral immunity against a recombinant protein without inducing inflammatory reponses. By fusing an amphipathic helical peptide to GFP increases the immunogenicity of GFP up to 1000 folds. This enhancement was correlated to the ability of amphipathic helical peptide in binding to cell membrane and causing lysosomal membrane permeabilization. We showed evidences that the amphipathic helical peptide may induces the delivery of antigen across lysosomal membrane into cytosol. Amphipathic helical peptide fusing provided a new pathway for stimulating immune responses against recombinant proteins.

Introduction

The challenge of developing a subunit vaccine focuses on two aspects: first, finding the right antigen that may serves as a countering target for host immune system; second, enhancing the specific host immune responses through various

mechanisms to a level that can counter the pathogen but will not causes harm to the host. The antigens for subunit vaccine comes from various component of the pathogen: polysaccharides, viral proteins that mediate infection, toxins that cause host morbidity or mortality. These antigen candidates are poor in activating host immune system and often requires the addition of adjuvant. The adjuvant according to FDA is a compound that is added to or used in conjuction with vaccine antigen to augment, potentiate or target specific immune response to antigen [1]. The adjuvant may be presented to immune system in different forms and activates immune responses through various pathways.

The amphipathic peptide is characterized by the propensity of a peptide being able to form both a hydrophilic and a hydrophobic surfaces and mediates the interactions between protein and membrane [2]. The M2 amphipathic helical (M2AH) peptide is the membrane anchor of type A influenza virus proton pump [3]. M2 proteins form a cross-membrane tetramer transporting protons need for endosome acidification and viral particle escape [3]. The M2AH resides on the cytoplasmic surface of host membrane and induces membrane curvature and scission in a cholesterol concentration dependent manner [4-6]. In a phospholipid bilayer containing cholesterol, the binding of M2AH induces membrane pit formation and a weaken lipid bilayer [7]. Certain M2AH variant is able to induce cholesterol dependent membrane leakage or membrane lysis [4]. In this study we have identified several amphipathic helical peptides that stimulated strong humoral immunity when they were fused with a model antigen, green fluorescent protein (GFP) and used in immunization.

Result

To test the effects of amphipathic helical peptide on the immunogenicity of a recombinant protein, we fused a peptide (AH2) from M2 protein of a type A

influenza virus strain A/TW/3355/97(H1N1) to green fluorescent protein (GFP). The fusion proteins were expressed and purified from *E. coli* strain BL21(DE3). The purified fusion proteins were used for the immunization of BALB/c mice by a prime and boost protocol. A variant of AH2 peptide (AH2M3) that contains three substitutions that disruted the membrane binding activity of AH2 was used as negative conrol. After immunization, the anti-GFP IgG titer were followed up to 6 months. Compared to His-GFP alone, the fusion protein contains functional amphipathic helical peptide is able to stimulate higher level of anti-GFP IgG titer (Figure 1B), where the membrane binding defective mutant, AH2M3 (Figure 1C), was unable to activate humoral immunity against GFP. The IgG subtype of the sera collected was then determined using subtype specific secondary antibodies. The result showed the titer of IgG1 is significantly higher than either IgG2a or IgG 2b, an indication that the immune response to tilted toward Th2 type (Figure 1D).

One potential explanation of amphipathic helical peptide mediated immunity boosting is by activating Toll Like Receptor (TLR) pathways, the major mechanism for boosting recombinant protein antigenicity by adjuvants. To test this hypothesis, we collected the mouse plasma 2 hour after intramuscular injection of either PBS, GFP, AH2-GFP, or TLR5 ligand, flagellin, and examined the expression of inflammatory cytokines, IL-6 and MCP-1. IL-6 and MCP-1 are cytokines that secreted by macrophage after activation of TLR pathways by invading pathogens or adjuvants. The flagellin is the strutural component of bacterial flagellum that control microbe movement and the ligand for TLR5. The results showed a dose dependent induction of IL-6 and MCP-1 expression by injected recombinant flagellin (Figure 2A, 2B). But not when the mice were injected with His-GFP or AH2-GFP recombinant proteins. These result suggest that the activation of humoral immunity by AH2-GFP is independent from the TLR signaling pathways, instead, the activity of AH2-GFP is correlated with its ability to bind plasma membrane.

To trace the transportation of AH2-GFP fusion proein after binding to plasma membrane, we incubated purified AH2-GFP fusion protein with cultured MDCK cells for four hours and evaluate whether AH2-GFP will be endocytosed into cell. The confocal images showed the endocytosed AH2-GFP in vesicle-like structure (Figure

3A). To trace the transportation of endocytosed AH2-GFP, we conjugated AH2 peptide onto the surface of gold nanoparticle (G-NP) and use transmissive electronic microscope to trace the tansport of G-NP. The cultured cell was either incubated with G-NP for 4 hours (Figure 3B-C)or 4+20 hours (Figure 3D-E) before been washed and processed for TEM imaging. The results showed that four hours post G-NP binding to plasma membrane, G-NP containing membrane (marked by arrow) was transported to multivesicle body (MVB), an organelle for membrane protein sorting, or lysosome (membrane rich and electron dense vesicle, labled L). In 4+20 hours post incubation, many G-NP was observed in enlarged lysosome (L) and many within permeabilized membranes (PL). Some of the enlarged lysosome were shown with broken membrane possibilly due to the AH2 peptide conjugated G-NP and some aggregated G-NP can be observed been released into cytoplasm (marked by arrow head). These results suggest the fusion of GFP with an amphipathic helical peptide not only mediates the binding of fusion protein onto plasma membrane, but also mediate the transport and delivery of fusion protein into cytoplasm through permeabilized lysosome.

Amphipathic helical peptide play multple roles in the protein-membrane interactions, including membrane anchorage, inducing membrane curvature and membrane lysis[2,8]. To evaluate whether the AH2 peptide possess membrane lysis activity as implicated in Figure 3C, the synthetic AH2, AH2M3, and Udorn peptides in increasing concentrations were applied to cultured Madin-Darby canine kidney (MDCK) cells. The positive control Udorn peptide, a M2 AH peptide that was derived from the influenza strain A/Udorn/72, has been shown to induce membrane leakage in artificial liposome that containes low percentage cholesterol in an in-vitro assay [4]. The effect of synthetic peptides on the viability of cultured MDCK cells was determined by flow cytometry for cells undergoing apoptosis and MTT assay for cells with metabolic activity. The results suggested 20% of the MDCK cells incubated with Udorn peptide became apoptotic at peptide concentration of 10 μM and the percentage of apoptotic cells increased with elevated peptide concentration (figure 4A). This result is in agreement with previous study from Lamb's group [4]. In

contrast, the percentage of MDCK cells undergoing apoptosis when treated with AH2 peptide concentration up to 100 μM was not significantly different from those treated with PBS. In MTT assay, the mitochondrian dehydrogenase enzyme activity of cells treated with Udorn peptide dropped significantly compared to cells treated with AH2 peptide in all three peptide concentrations. Whereas the viabiilty of MDCK cells treated with AH2 peptide only became significantly different from PBS control when the peptide concentration reached 100 μM. These results suggests the AH2-fusion protein have to reach 100 μM (3.5 mg/ml) to induce a minor reduction in cell viability.

To test whether AH2 mediated activation of humoral immunity is a particular phenomenum or a common feature of amphipathic helical peptide, we replaced AH2 peptide with published AH peptides from either NSP1 of Semliki Forest virus (NSP1), G-protein coupled protein kinase 5 (GRK5), or the fusion peptide of Hemagglutinin (HAfp23). These fusion proteins were expressed and purified under the same conditions as AH2-GFP and were used for mice immunization by a two doses protocol with a 14 days gap. The result showed all the fusion peptides tested were able to boost the anti-GFP IgG titer after mice immunization by fusing to GFP by a magnitude about 1000 folds. This increase in antibody titer against a recombinant protein is significant when compared to the adjuvants that have been used to boost the antigenicity of a subunit vaccines. The use of Alum salt increased the anti-GFP IgG titer by 10s folds and TLR4 ligand MPLA also had similar activities but not as significant as fusing to GRK5 peptide (Figure 5B).

Discussion

The study results indicates the AH peptie fusion enhanced the antibody production against model antigen, GFP. This increase is significant since the comparison with known adjuvants suggest AH peptide fusion is more effective in stimulating antibody production. Adjuvant that activates Th1 type immune responses activates CD4+ T cell and IgG2a expression whereas adjuvant that activates Th2 pathway

induces IgG1 expression through CD8+ T cell. We have not tested whether AH peptide also activates cellular immunity against GFP expressing cells, but the IgG subclass indicates the balanced activation of both T helper type 1 (Th1) and Th2 pathways.

In our results, binding of AH2 peptide conjugated G-NP caused permeabilization of lysosome membrane but not the plasma membrane. In an in vitro membrane binding study, the M2AH peptide (the same Udorn peptide as in this study) binding induces membrane leakage in a synthetic liposome when the liposome membrane contained low percentage cholesterol but not when membrane contained high cholesterol [4]. Since the distribution of choleserol in mammalian cell is organelle dependent, it is rich in multiple vesicle body (MVB) and plasma membrane but low in lysosome [9], so it is likely that the AH2 peptide only induces membrane leakage when been sorted into lysosome. Another study suggested M2AH binds cholesterol through the aromatic side chains of F47 [5] and the binding of M2AH weaken lipid bilayer by introducing membrane pit [7]. So the binding of AH2 peptide likely introduces cholseterol depleted membrane pit and causes lysosomal membrane leakage. This mechanism is similar to the QS-21, the main component of several clinically approved adjuvants, which induces endocytosis and lysosome pore formation through binding to cholesterol [10]. Other adjuvants that activate immunity through lysosomal leakage including Alum salt [11,12].

The AH2-GFP fusion protein immuization did not induce acute expression of IL-6 or MCP-1, two inflammatory cytokines. There are two potential explanations for this result. First, as in the QS-21 study suggested, the QS-21 effect on the NF-kB pathway and its down stream effects, including IL-6 expression is depend on lysosomal maturation which takes longer time than TLR signaling. So the time points (2hrs post injection) used to determine cytokine level in this study maybe too early to catch the IL-6 expression induced by lysosomal leak and its downstream NF-κB activation. One study that worth notice was the delayed induction of IL-6 and other inflammatory cytokines after immunization with Alum salt adjuvanted antigen [13]. Another potential explanation is the distinct pathways that leading to NF-kB

singaling and IgG antibody titer induction activated by QS-21[10]. In this aspect, the AH2 peptide plays a similar role as QS-21 or they share the same ability to destabilize lysosomal membrane. Applying QS-21 alone causes cell apoptosis, so it is often formulated with cholesterol and phospholipid to reduce cytotoxicity [14-16]. But the formulation of a protein based vaccine in a oil-in-water nanoemulsion adjuvant may cause instability of antigen when it is stored at ambient temperature and it required either lyophilization [17] or spray drying [18] after adding excepients to achieve long-term thermostability. In comparison, protein nanoparticles assembled by amphipathic helical peptide is self-adjuvanted and can be stored as ready to use doses at ambient temperature [19,20].

In this study, several known amphipathic helical peptides were used to evaluate their effects on GFP antigenicity. The GRK5-AH is derived from the C-terminal AH peptide of G protein-coupled protein kinase 5 (GRK5) [21], together with N-terminal helical basic peptide they anchoring the GRK5 protein onto plasma membrane[22]. The NSP1-AH is adopted from the the replicase of Semliki forest virus, nsP1 [23,24]. This peptide is conserved in replicases from all alphaviruses including Chikungunya virus [25]. The HAfp23-AH is the fusion peptide of hemagglutinin from infleunza virus that induces membrane curvature and fusion through two tightly packed hairpin helix buried in lipid bilayer [26]. There is no similarity in peptide sequences among four peptides presented in this study or shared mechanism that can fully explain their activity in boosting antigenicity. The common features is the tendency to interact with phospholipid membrane through hydrophobic face. One potential explanation comes from our recent work [19]. When the Cys8 from a modified M2AH peptide, LYRRLE, was replaced by serine, the substitution caused the hydrolysis of subunit protein the particle size increased from 23 nm to 600 nm, suggesting the particle is a losely packed aggregation through hydrophobic interaction [19]. So the activity of AH peptides in enhancing anti-GFP IgG may reside in the its ability to form a random aggregation after fusing with GFP. Other example of GFP fusion protein forming aggregated megastructure and gained high antigenicity has been reported when GFP was fused with a N-terminal domain of polyhedrin protein [27]. But the replacement of GFP with known vaccine antigen in this megastructure is

209 difficult because of the interuption in protein folding when protein is packed closely.
210 In conclusion, the fusion with amphipathic helical peptide provide a novel
211 mechanism for stimulating immunity and maybe applied in other antigens other
212 than GFP if the following goals can be achieved: extended protein stability, efficient
213 incorporation of heterologous protein and high specificity to target cell.
214
215 Materials and methods

216 **Expression and purification of endotoxin free protein**

217 The pET28a vector encoding target protein was transformed into BL21 (DE3) using
218 heat shock. The procedure for heat shock transformation is as follow. Day 1 at 3pm,
219 plasmid of 1ng was mixed with 50 µl thawed competent cell, BL21(DE3), and
220 incubates on ice for 10 minutes before 42 °C heat shock for 40 seconds. After heat
221 shock, mixture was kept on ice for 1 minute before adding 1ml LB and then shakes
222 at 220 rpm at 37 °C for 1 hour. Then bacteria were spun down at 13000 rpm for 1
223 minute. The bacteria pellet was re-suspended in 100 µl LB and plated on LB plate
224 with 100 µg/ml ampicillin and incubated at 37 °C. Day 2, at 10 am, there should be
225 less than 100 colonies on the plate. Pick one colony and inoculate 3ml LB/ampicillin
226 culture and incubated at 37℃/225 rpm. By 12 am, the 3ml culture was transferred
227 to 500ml LB/ampicillin media and the growth of culture monitored by
228 spectrophotometer. When OD600 reached 0.5-0.7, 1 mM IPTG was added into the
229 culture to induce protein expression. The culture was harvested 3 hours after
230 protein induction. Bacteria were spun down by centrifuge at 5000 rpm for 10
231 minutes. Supernatant were removed and the pellet kept for further procession.

232 **Protein purification**

233 Buffer for protein purification and gel filtration: 20 mM $NaPO_4$, pH 7.4, 300 mM NaCl
234 (GF buffer). For Ni-NTA resin purification: 5 mM Imidazole in GF for bacteria lysis
235 (Lysis buffer), 10 mM Imidazole in GF for wash (Wash buffer), 200 mM Imidazole in

GF for protein elution (Elution buffer). Bacteria pellet from 500 ml LB culture was re-suspended in 40 ml Lysis buffer by vortex and then lysed using ultrasonic sonicator (Misonix 3000) at 10S on/5S off cycles for 5 minutes. The re-suspended bacteria were kept in icy water during sonication. Insoluble debris was removed by centrifugation in 10000 rpm for 10 minutes using Sorval SS34 rotor at 4 ^{o}C. Supernatant containing target protein was passed through a polypropylene column contained 2ml Ni-NTA resin from Qiagen. After target protein binded to the Ni-NTA resin, the column was washed by 10 bed volume of wash buffer (20 ml). After wash, the target protein was then eluted using 5ml elution buffer. Target protein purified using Ni-NTA resin was further purified using Gel filtration column from GE (HiLoad 16/600 Superdex 200 pg) on AKTA prime.

Size exclusion chromatography

Three programs were setup for the purification of proteins in study. Program 30: For gel filtration purification of target protein. Program 33: for onsite cleaning of HiLoad 16/600 superdex 200 pg using 120ml 0.5M NaOH. Flow rate is 0.8ml/minutes. Program 34: for equilibrate column after onsite cleaning using 150ml GF buffer. Column was washed after two protein purifications. A 5ml sample loop was connected to the machine, AKTA prime, for holding protein sample. Sample loop is first flushed using 25 ml GF buffer to remove residual protein in previous purification. Before loading target protein into the sample loop, additional 0.5ml GF buffer was added into the Ni-NTA purified protein. Protein solution was placed into a 5 ml syringe and loaded into the sample loop. Glass tubes in the corresponding fractions of target protein eluted were replaced with new tubes every time before the purification. All the buffers to be used in the gel filtration experiment were filtered through a 0.2 μm filter unit for sterilization and removal of impurity. These buffers were further degassed by vacuum for 10 minutes. FPLC

Fractions contained target proteins as monitored by UV280 were collected and pooled together. The pooled protein solution was concentrated by 2nd Ni-NTA column with same bed volume as first one. After the protein was eluted from 2nd Ni-NTA column, protein concentration was determined by BCA method. Two fractions with highest protein concentration were pooled and dialyzed against 1L PBS over night. After dialysis, endotoxin contaminant was removed using EndotoxinOUT™ resin from G-Bioscience. The polypropylene column was filled with 4ml EndotoxinOUT™ resin and washed with 5 bed volume of 1% sodium deoxycholate in LAL Reagent Water (LRW), 5 bed volume of LRW and 5 bed volume of PBS/LRW before loading 1.5ml target protein. After complete loading of the protein, column was placed in cold room for 1 hour for complete absorption of endotoxin by resin. Protein was eluted using step wise addition of first fraction 0.5 ml and later fractions 1 ml of PBS. Protein was eluted in the 3rd to 6th fractions.

LAL assay

Endotoxin level was determined using PYROTELL-T LAL provided by Associate of Cape Cod. Each LAL reagent supplied in lyophilized powder is first dissolved in 5ml LRW and then aliquot into small volume and kept in -80 °C. In a typical turbidity assay using PYROTELL-T, 100 µl of sample including endotoxin standard were applied in a microplate. The reaction kinetic was measured using victor3 fluorescence reader by OD405 at 37 °C. The time-lapse between each reading was 70 seconds and the reading was repeated for 60 times. The time needed for a reaction to reach a difference of 0.1 in OD405 between sample and blank was recorded and compared to endotoxin standard to determine the endotoxin unit in a sample. The log of endotoxin activity was plotted against time (seconds) to reach a difference of 0.1 in OD405; a logarithmic trend line is used as standard curve. The identified endotoxin activity in a protein sample was further combined with protein

288 concentration, as determined by BCA assay, to determine specific endotoxin activity,
289 EU/mg. The upper limit of specific endotoxin activity in all the protein samples was
290 5 EU/mg.

291

292 **Animal Immunization**

293 The C57BL/6 SPF mice used in immunization procedures were between 6 and 8
294 weeks and provided by BioLasco Taiwan. Without anesthetization, mouse was bled
295 from tail by clipping away 2-3mm tail. Blood was collected using pipetman with
296 occasional massaging on the tail. About 100 µl blood was collected from each
297 bleeding. Blood was left at RT for 2 hours before centrifugation at 2000 rpm for 10
298 minutes in a microcentrifuge, and serum was collected in a microtube. Remained
299 lymphocytes were removed by centrifugation at 2000 rpm for 10 minutes in a
300 microcentrifuge. Serum was stored in -80 ^{o}C before use in an ELISA assay. Mouse
301 tail bleeding is stopped by heated soldering iron while pressing the tail tip between
302 fingers. For primary immunization, 20 µg purified protein was injected
303 intramuscularly in the thigh of hind limb. Blood was bled 14 days post
304 immunization from tail and booster dose with same amount of purified protein was
305 injected by same procedure.

306

307 **ELISA for determining antibody titer**

308 The anti-GFP IgG titer was deteremined by coating GFP protein at a concentration of
309 10 µg/ml. The procesdures of ELISA assay following the standard protocol.
310 Secondary Ab (HRP conjugated Goat anti-mouse Ab) was used as 5000 folds
311 dilution by blocking buffer. Coating buffer contains 0.2 M Carbonate/Bicarbonate
312 buffer at pH 9.4. The washing buffer contains 0.05% Tween 20 in 1X PBS. Blocking

313 buffer contains 1% BSA in washing buffer and the stop buffer contains 2M sulfuric
314 acid.

315

316 **GFP fusion protein binding assay**

317 The GFP fusion protein binding activity was tested by first plating $4x10^4$ MDCK cells
318 on one well of a 96 well plate, each sample was tested in quadruplicate. On second
319 day, 200 µg/ml of GFP fusion protein was added into the culture media and
320 incubated for 4 hours. After incubation, media was removed and washed with 200
321 µl of PBS for three times. The amount of GFP fusion protein bound/internalized was
322 determined by a fluorometer.

323

324 **Plasma cytokine determination**

325 For detecting blood cytokine level, mice were first intramuscularly injected with
326 experimental proteins. Two hours after injection, the mice were anaesthetized
327 before collecting blood through cardiac puncture with a syringe preloaded with 10
328 µl of 0.5M Na_2EDTA. Blood collected were centrifuged at 2000 rpm for 20 minutes
329 at a tabletop microcentrifuge. Plasma collected was aliquoted into 20 µl fractions
330 and snap frozen on dry ice. The plasma cytokine level was determined by sandwich
331 ELISA with standard from eBioscience, USA. IL-6 level was detected using Mouse IL-
332 6 ELISA Ready-SET-Go! (Cat#88-7064, eBioscience, USA). MCP-1 was detected
333 using Mouse CCL2 (MCP-1) ELISA Ready-SET-Go! Kit [28-7391, eBioscience, USA]. The
334 detecting procedures followed the manufacturer's standard protocol.

335

336 **Cell apoptosis assay by flow cytometer and MTT assay**

MDCK cells were first plated on 6 well plates at 3x10E5 cell/well. Twenty-four hours after plating, peptides were applied to 10 μM, 30 μM, or 100 μM concentration and cells were incubated for 24 hours before harvest by trypsin digestion. The suspended cells due to apoptosis were collected by centrifuging the culture media at 1000 rpm for 5 minutes. The cells collected from trypsin digestion and cultured media were combined and cells were fixed in 3 ml 70 % ethanol overnight in -20 ^{o}C freezer. After fixation, cells were washed and resuspended in 1 ml PBS and stained by SYTOX AADvanced Dead Cell Stain kit (Thermo Fisher Scientific Inc.) in the presence of 100 μg RNaseA for 30 minute in 4 degree cold room before analysis by flow cytometer (Calibur BD). The sub-G1 fraction was calculated and designated as apoptotic cells. For MTT assay, MDCK cells were plated at 96 well plateat 1x10E4 cell/well. Twenty-four hours after plating, peptide was added to reach concentration of 10 μM, 30 μM, or 100 μM and cell were incubated for 24 hours and media removed and replaced with 50 μl serum free media and 50 μl MTT solution. After incubation at 37 ^{o}C for 3 hours, 150 MTT solvent was added and the plate was shaked for 15 minutes and then read the absorbance at OD570.

Transmission electronic microscope

Madin-Darby canine kidney (MDCK) cells were seeded on ACLAR EMBEDDING film in a 6 well plate at density of $3x10^5$ cell per well. After overnight culturing, part of the media were removed to leave 0.5ml of culture media before adding 50 μl of 10 nm gold nanoparticle conjugated with AH2 peptide. The concentration of AH2 conjugated 10 nm gold nanoparticle used in this assay was $4.78x10^{12}$/ml. After 4 hours incubation, cells were washed in serum-free culture media at room temperature and fixed directly or cultured for additional 20 hrs before fixation. The fixation procedure was by covering the film in 2.5% glutaraldehyde/0.1% tannic

363 acid/0.1M cacodylate buffer, pH 7.2 at room temperature for 30 minutes. Then cells
364 were washed in 0.1M cacodylate buffer pH 7.2/0.2M sucrose/0.1% $CaCl_2$ for 5
365 minutes at room temperature. Afterward, cells were post-fixed in 1% OsO_4/0.1M
366 cacodylate buffer, pH 7.2 at room temperature for 30 minutes. Then cells were
367 washed with ddH_2O for three times, 5 minutes each in room temperature. Cells
368 were further stained with 1% uranyl acetate at room temperature for 30 minutes
369 before washed in ddH_2O for 3 times. Cell were then dehydrated and embedded in
370 EPON by polymerized at 60 ^oC for 24 hours. Embedded cells were then sectioned
371 for observation under transmission electronic microscope.
372
373
374
375

Figures

Figure 1

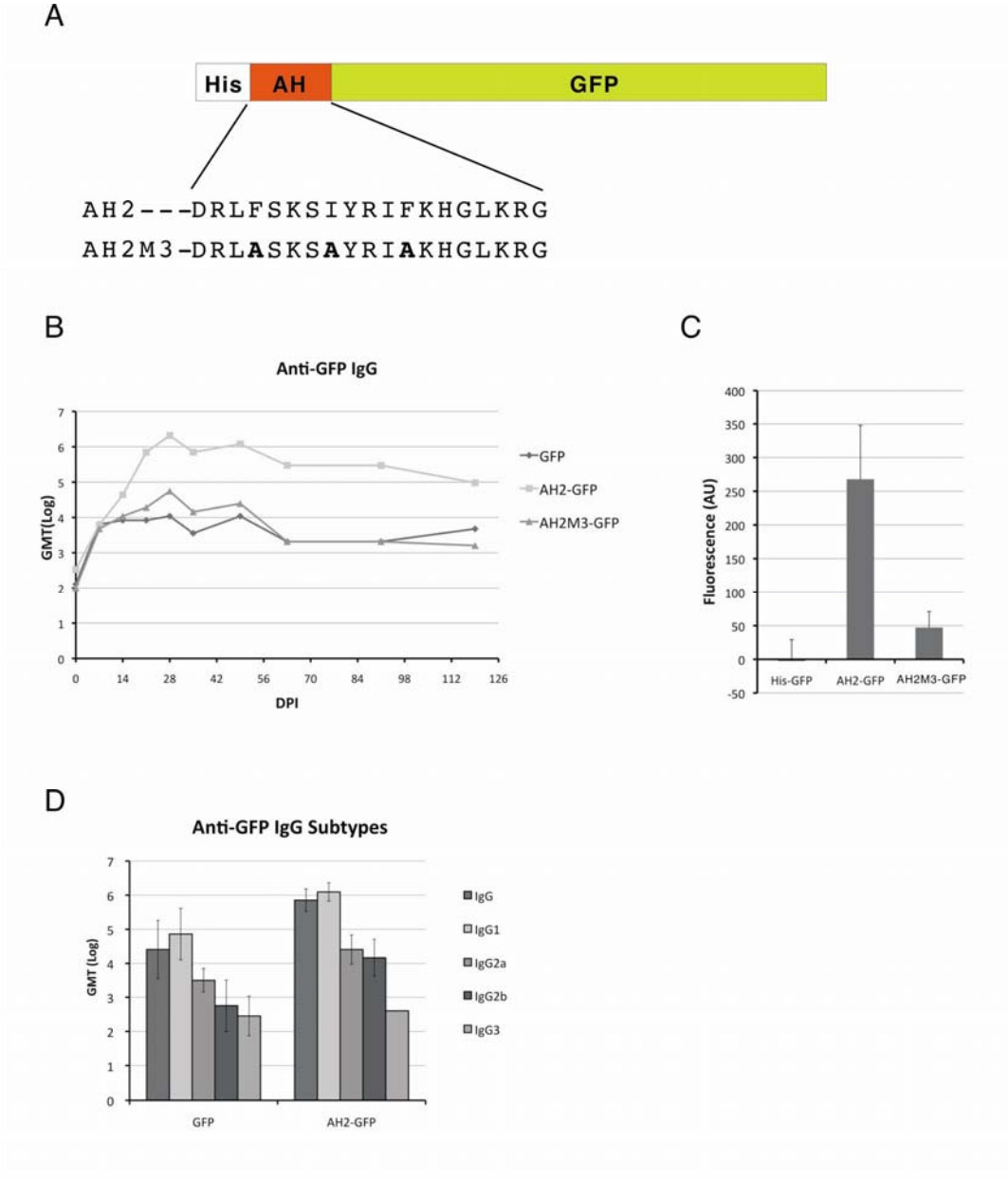

Figure 1. The effect of AH peptide mediated recombinant protein antigenicity enhancement. (A) The design of AH fusion protein was shown. The AH peptide from M2 protein of influenza virus strain A/TW/3355/97 H1N1 (AH2) was inserted between His-Tag and GFP. The amino-acid sequence of AH2 peptide and its

membrane binding mutant, AH2M3, were shown. (B) The change of anti-GFP IgG titers were determined by ELISA and followed for 4 months. Mice were immunized twice with 20 μg each of His-GFP, AH2-GFP or AH2M3-GFP at day 0 and day 14 by intramuscular injection. Sera for ELISA assay were collected every 7 days at first month, every 2 weeks up to second month and monthly up to fourth month. The anti-GFP IgG geometric mean titer was shown as GMT (Log) (N=5). (C) The membrane binding activity of fusion proteins was measured by incubating the fusion proteins with cultured MDCK cells for 4 hours and then washed with PBS for quantification under fluorometer. (D) The anti-GFP IgG subtypes of sera collected at day 28 after primary dose of His-GFP or AH2-GFP were determined. HRP conjugated goat anti-mouse IgG1, goat anti-mouse IgG2a, goat anti-mouse IgG2b and goat anti-mouse IgG3 secondary antibodies were used in the ELISA assay.

Figure 2

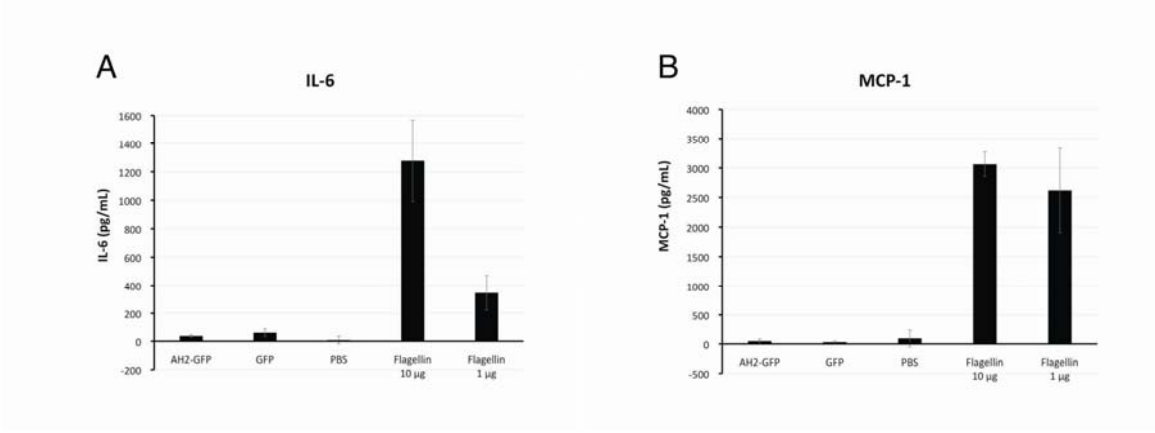

Figure 2. Detection of inflammatory cytokines level after antigen immunization. Mice were injected with either PBS, His-GFP, AH2-GFP, 10 μg flagellin or 1 μg flagellin and plasma were collected 2 hours post immunization for detection of A) IL-6 and B) MCP-1 by sandwich ELISA. (N=5).

403 Figure 3

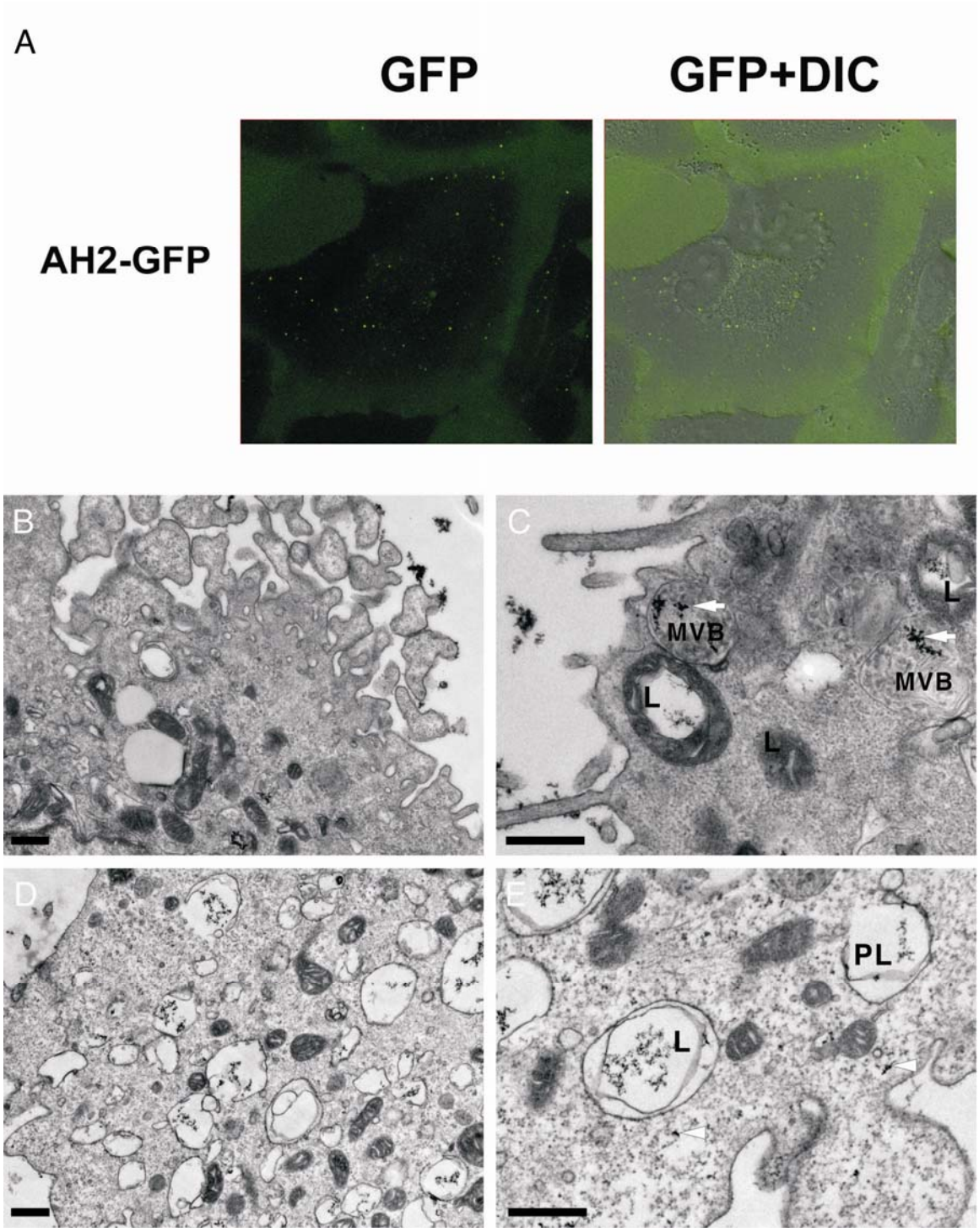

404

405 Figure 3. The binding and transportation of AH2-GFP and AH2 G-NP into cytoplasm

406 were examined under confocal fluorescence microscope or transmission electronic

407 microscope (TEM). (A) Purified AH2-GFP fusion protein was incubated with
408 cultured MDCK cell and non-binding protein was washed away after 4 hours
409 incubation then the location of internalized AH2-GFP was traced by confocal
410 fluorescence microscope. The transportation of AH2 peptide conjugated gold
411 nanoparticle (G-NP) was traced by TEM. The MDCK cell was incubated with G-NP for
412 either (B-C) 4 hours or (D-E) 4+20 hours before cell was fixed and embedded for
413 TEM imaging. The arrow points to the internalized G-NP in lysosome (L) or
414 permeabilized lysosome (PL) or multiple vesicle body (MVB). The arrowheads
415 pointed to the positions of released G-NP in cytoplasm. The length of the scale bar is
416 500 nm.

417 Figure 4

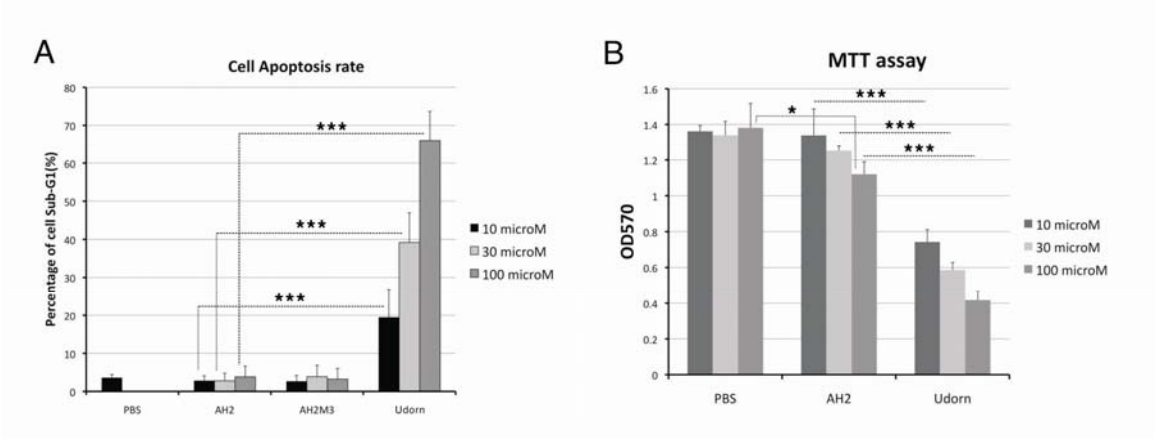

418

419 Figure 4. Evaluating the cytotoxic effects of amphipathic helical peptides by Flow
420 cytometry and MTT assay. (A) The percentage of cells in apoptosis after been
421 exposed to AH peptide was measured by Flow cytometry. MDCK cell was incubated
422 with 10 microM, 30 microM or 100 microM of synthetic peptides for 24 hrs and then
423 the cell was harvested for detecting apoptotic cells using nuclei staining. (B) The
424 viability of MDCK cells after been incubated with synthetic peptides for 24 hours
425 was meaured by MTT assay. The AH2 peptide or Udorn peptide were added into the

culture media to make increasing concentrations of 10 microM, 30 microM or 100 microM. (*** P≤0.001, * P≤0.05)

Figure 5

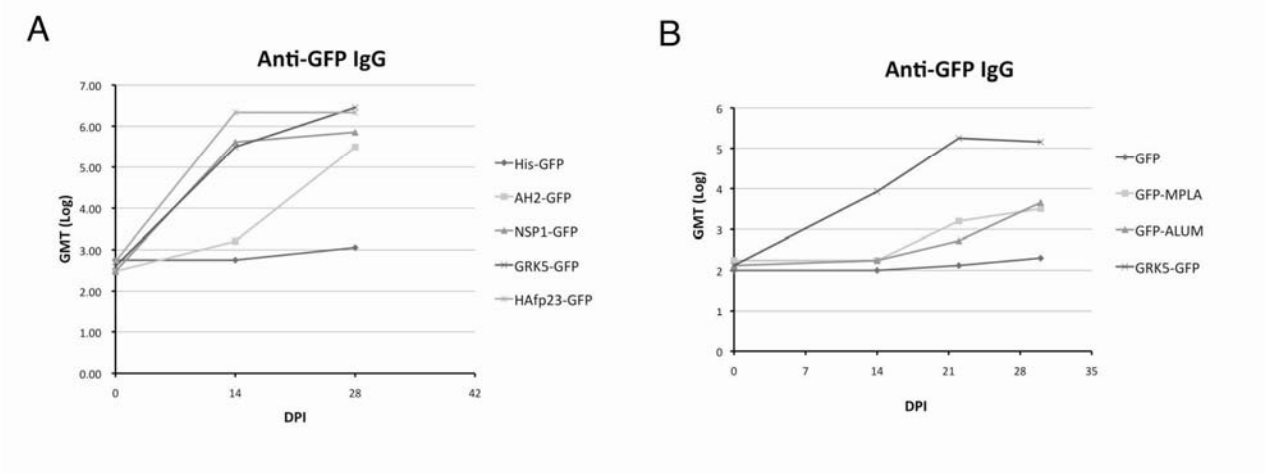

Figure 5. The evaluation of different amphipathic helical peptides in enhancing GFP antigenicity and the comparison with other adjuvants. (A) The AH peptides from M2 protein of H1N1 influenza virus (AH2-GFP), Semliki Forest virus replicase nsP1 (NSP1-GFP), G-protein coupled kinase 5 (GRK5-GFP), Fusion hairpin peptide of Hemaglutinin (HAfp23-GFP) were fused with GFP and the fusion proteins were purified and used for mice immunization in a two doses protocol. The anti-GFP IgG titer was determined from sera collected 14 days post immunization. (B) The comparison of GFP antigenicity boosting by either GRK5 peptide (GRK5-GFP), Alum salt (GFP-ALUM), or MPLA (GFP-MPLA) in a two doses immunization protocol. The anti-GFP IgG titer was determined using ELISA. (N=5)

References

1. FDA. Regulatory Considerations in the Safety Assessment of Adjuvants and Adjuvanted Preventive Vaccines

2. Almeida, P.F. Membrane-active peptides: binding, translocation, and flux in lipid vesicles. *Biochim Biophys Acta* **2014**, *1838*, 2216-2227, doi:10.1016/j.bbamem.2014.04.014 [doi].
3. Pinto, L.H.; Lamb, R.A. The M2 proton channels of influenza A and B viruses. *J Biol Chem* **2006**, *281*, 8997-9000, doi:10.1074/jbc.R500020200 [doi].
4. Rossman, J.S.; Jing, X.; Leser, G.P.; Lamb, R.A. Influenza virus M2 protein mediates ESCRT-independent membrane scission. *Cell* **2010**, *142*, 902-913, doi:10.1016/j.cell.2010.08.029 [doi].
5. Martyna, A.; Bahsoun, B.; Madsen, J.J.; Jackson, F.S.J.S.; Badham, M.D.; Voth, G.A.; Rossman, J.S. Cholesterol Alters the Orientation and Activity of the Influenza Virus M2 Amphipathic Helix in the Membrane. *J Phys Chem B* **2020**, *124*, 6738-6747, doi:10.1021/acs.jpcb.0c03331 [doi].
6. Elkins, M.R.; Williams, J.K.; Gelenter, M.D.; Dai, P.; Kwon, B.; Sergeyev, I.V.; Pentelute, B.L.; Hong, M. Cholesterol-binding site of the influenza M2 protein in lipid bilayers from solid-state NMR. *Proc Natl Acad Sci U S A* **2017**, *114*, 12946-12951, doi:10.1073/pnas.1715127114 [doi].
7. Pan, J.; Dalzini, A.; Song, L. Cholesterol and phosphatidylethanolamine lipids exert opposite effects on membrane modulations caused by the M2 amphipathic helix. *Biochim Biophys Acta Biomembr* **2018**, *1861*, 201-209, doi:10.1016/j.bbamem.2018.07.013 [doi].
8. Tossi, A.; Sandri, L.; Giangaspero, A. Amphipathic, alpha-helical antimicrobial peptides. *Peptide Science* **2000**, *55*, 4-30, doi:10.1002/1097-0282(2000)55:1<4::aid-bip30>3.0.co;2-m.
9. Möbius, W.; van Donselaar, E.; Ohno-Iwashita, Y.; Shimada, Y.; Heijnen, H.F.; Slot, J.W.; Geuze, H.J. Recycling compartments and the internal vesicles of multivesicular bodies harbor most of the cholesterol found in the endocytic pathway. *Traffic* **2003**, *4*, 222-231, doi:10.1034/j.1600-0854.2003.00072.x [doi].
10. Welsby, I.; Detienne, S.; N'Kuli, F.; Thomas, S.; Wouters, S.; Bechtold, V.; De Wit, D.; Gineste, R.; Reinheckel, T.; Elouahabi, A.; et al. Lysosome-Dependent Activation of Human Dendritic Cells by the Vaccine Adjuvant QS-21. *Front Immunol* **2017**, *7*, 663, doi:10.3389/fimmu.2016.00663 [doi].
11. Brojatsch, J.; Lima, H.; Kar, A.K.; Jacobson, L.S.; Muehlbauer, S.M.; Chandran, K.; Diaz-Griffero, F. A proteolytic cascade controls lysosome rupture and necrotic cell death mediated by lysosome-destabilizing adjuvants. *PLoS One* **2014**, *9*, e95032, doi:10.1371/journal.pone.0095032 [doi].
12. Jacobson, L.S.; Lima, H., Jr.; Goldberg, M.F.; Gocheva, V.; Tsiperson, V.; Sutterwala, F.S.; Joyce, J.A.; Gapp, B.V.; Blomen, V.A.; Chandran, K.; et al. Cathepsin-mediated necrosis controls the adaptive immune response by Th2 (T helper type 2)-associated adjuvants. *J Biol Chem* **2013**, *288*, 7481-7491, doi:10.1074/jbc.M112.400655 [doi].
13. Ito, T.; Inouye, K.; Fujimaki, H.; Tohyama, C.; Nohara, K. Mechanism of TCDD-induced suppression of antibody production: effect on T cell-derived cytokine production in the primary immune reaction of mice. *Toxicol Sci* **2002**, *70*, 46-54, doi:10.1093/toxsci/70.1.46 [doi].

14. Duewell, P.; Kisser, U.; Heckelsmiller, K.; Hoves, S.; Stoitzner, P.; Koernig, S.; Morelli, A.B.; Clausen, B.E.; Dauer, M.; Eigler, A.; et al. ISCOMATRIX adjuvant combines immune activation with antigen delivery to dendritic cells in vivo leading to effective cross-priming of CD8+ T cells. *J Immunol* **2011**, *187*, 55-63, doi:10.4049/jimmunol.1004114 [doi].
15. Baz Morelli, A.; Becher, D.; Koernig, S.; Silva, A.; Drane, D.; Maraskovsky, E. ISCOMATRIX: a novel adjuvant for use in prophylactic and therapeutic vaccines against infectious diseases. *J Med Microbiol* **2012**, *61*, 935-943, doi:10.1099/jmm.0.040857-0 [doi].
16. Wilson, N.S.; Yang, B.; Morelli, A.B.; Koernig, S.; Yang, A.; Loeser, S.; Airey, D.; Provan, L.; Hass, P.; Braley, H.; et al. ISCOMATRIX vaccines mediate CD8+ T-cell cross-priming by a MyD88-dependent signaling pathway. *Immunol Cell Biol* **2012**, *90*, 540-552, doi:10.1038/icb.2011.71 [doi].
17. Kramer, R.M.; Archer, M.C.; Orr, M.T.; Dubois Cauwelaert, N.; Beebe, E.A.; Huang, P.D.; Dowling, Q.M.; Schwartz, A.M.; Fedor, D.M.; Vedvick, T.S.; et al. Development of a thermostable nanoemulsion adjuvanted vaccine against tuberculosis using a design-of-experiments approach. *Int J Nanomedicine* **2018**, *13*, 3689-3711, doi:10.2147/IJN.S159839 [doi].
18. Gomez, M.; Archer, M.; Barona, D.; Wang, H.; Ordoubadi, M.; Bin Karim, S.; Carrigy, N.B.; Wang, Z.; McCollum, J.; Press, C.; et al. Microparticle encapsulation of a tuberculosis subunit vaccine candidate containing a nanoemulsion adjuvant via spray drying. *Eur J Pharm Biopharm* **2021**, *163*, 23-37, doi:10.1016/j.ejpb.2021.03.007 [doi].
19. Kan, M.-C. The thermostability of a VADEX-Pro based protein nanoparticle. *bioRxiv* **2023**.
20. Wong, T.-T.; Liou, G.-G.; Kan, M.-C. A Thermal-Stable Protein Nanoparticle That Stimulates Long Lasting Humoral Immune Response. *Vaccines* **2023**, *11*, 426.
21. Thiyagarajan, M.M.; Stracquatanio, R.P.; Pronin, A.N.; Evanko, D.S.; Benovic, J.L.; Wedegaertner, P.B. A predicted amphipathic helix mediates plasma membrane localization of GRK5. *J Biol Chem* **2004**, *279*, 17989-17995, doi:10.1074/jbc.M310738200 [doi.
22. Ding, B.; Glukhova, A.; Sobczyk-Kojiro, K.; Mosberg, H.I.; Tesmer, J.J.; Chen, Z. Unveiling the membrane-binding properties of N-terminal and C-terminal regions of G protein-coupled receptor kinase 5 by combined optical spectroscopies. *Langmuir* **2014**, *30*, 823-831, doi:10.1021/la404055a [doi].
23. Lampio, A.; Kilpeläinen, I.; Pesonen, S.; Karhi, K.; Auvinen, P.; Somerharju, P.; Kääriäinen, L. Membrane binding mechanism of an RNA virus-capping enzyme. *J Biol Chem* **2000**, *275*, 37853-37859, doi:10.1074/jbc.M004865200 [doi].
24. Spuul, P.; Salonen, A.; Merits, A.; Jokitalo, E.; Kääriäinen, L.; Ahola, T. Role of the amphipathic peptide of Semliki forest virus replicase protein nsP1 in membrane association and virus replication. *J Virol* **2007**, *81*, 872-883, doi:10.1128/JVI.01785-06 [doi].
25. Zhang, K.; Law, Y.S.; Law, M.C.Y.; Tan, Y.B.; Wirawan, M.; Luo, D. Structural insights into viral RNA capping and plasma membrane targeting by

Chikungunya virus nonstructural protein 1. *Cell Host Microbe* **2021**, *29*, 757-764 e753, doi:10.1016/j.chom.2021.02.018 [doi].

26. Smrt, S.T.; Draney, A.W.; Lorieau, J.L. The influenza hemagglutinin fusion domain is an amphipathic helical hairpin that functions by inducing membrane curvature. *J Biol Chem* **2015**, *290*, 228-238, doi:10.1074/jbc.M114.611657 [doi].

27. Cruz-Reséndiz, A.; Zepeda-Cervantes, J.; Sampieri, A.; Bastián-Eugenio, C.; Acero, G.; Sánchez-Betancourt, J.I.; Gevorkian, G.; Vaca, L. A self-aggregating peptide: implications for the development of thermostable vaccine candidates. *BMC Biotechnol* **2020**, *20*, 1, doi:10.1186/s12896-019-0592-9 [doi].

28. .